Growth characteristics of sputter-deposited UPt_3 thin films

To cite this article: M Huth *et al* 1996 *J. Phys.: Condens. Matter* **8** 8777

View the article online for updates and enhancements.

Growth characteristics of sputter-deposited UPt$_3$ thin films

M Huth†, S Reber†, C Heske‡, P Schicketanz†, J Hessert†, P Gegenwart§ and H Adrian†

† Institut für Physik, Johannes Gutenberg-Universität Mainz, 55099 Mainz, Germany
‡ Experimentelle Physik II, Universität Würzburg, 97074 Würzburg, Germany
§ Institut für Festkörperphysik, Technische Hochschule Darmstadt, 64289 Darmstadt, Germany

Abstract. Thin films of the heavy-fermion superconductor UPt$_3$ were deposited on various substrate materials in various orientations by means of a quasi-multilayer sputter process. Strongly (0001)-textured growth of the hexagonal compound was found for a uranium content in the range of 23% to 28% on sapphire (10$\bar{1}$2), LaAlO$_3$(111) and SrTiO$_3$(111) with perfect in-plane order on the latter substrate material. Atomic force microscopy and scanning electron microscopy revealed a Vollmer–Weber-like growth mode resulting in the development of large compressive strain in films on SrTiO$_3$(111). As a result the electronic transport properties—in particular the temperature dependence of the resistivity—were strongly renormalized. Strong deviations from the typical heavy-fermion characteristics known from UPt$_3$ bulk samples were found in films on SrTiO$_3$ with residual resistance ratios $\rho(300\,\text{K})/\rho_0$ up to 930 and a significantly reduced superconducting transition temperature of 130 mK.

1. Introduction

Among the heavy-fermion systems the superconducting compounds are of special interest. This is due to the fact that the strong local Coulomb repulsion favours a superconducting order parameter that is not subject to an s-wave symmetry [1]. In particular, experiments on UPt$_3$ show clear evidence for an order parameter of non-conventional structure (for recent reviews see [2, 3]). The B–T phase diagram in the Shubnikov phase is well established within an experimental temperature resolution of 17 mK revealing three superconducting phases that meet in a tetracritical point for the main crystallographic directions $B \parallel c$, $B \perp c$ and $\angle(B, c) = 45°$ [4]. The low-temperature power-law behaviour of the specific heat [5, 6] and the anisotropy in sound propagation experiments [7] corroborate the assumption of an equatorial line node in the energy gap on the Fermi surface. The suppression of the double transition in specific heat experiments under hydrostatic pressure [8, 9] corresponds to an almost parallel disappearance of the antiferromagnetic order as was shown in neutron scattering experiments [10]. As a consequence of these experimental findings several models for the underlying superconducting order are discussed. In the strong-spin–orbit-coupling limit, Sauls [2] favour a two-dimensional orbital representation coupled to a symmetry-breaking field whereas Chen and Garg suggest two one-dimensional representations which are nearly degenerate [12]. A spin-triplet order parameter in a one-dimensional orbital representation without spin–orbit coupling in the pairing channel is suggested by Machida and Ozaki [11]. In order to decide which of these models are realized in UPt$_3$ several key experiments are suggested. One of these experiments is based on the phase relationship between the critical current and the applied magnetic flux in a SQUID constructed from

two junctions between UPt_3 and a conventional superconductor (see e.g. [2]). Analogous experiments have been persued on the high-T_c superconductors in order to test for a broken reflection symmetry ($d_{x^2-y^2}$ order parameter) [13]. Experimentally, even the existence of a Josephson current between two pieces of UPt_3 or between UPt_3 and a conventional superconductor remains to be proven. This represents one of the motivations for the preparation of UPt_3 as thin films which is the main concern of the present paper. By lithographical patterning of the films for the junction preparation it is possible to avoid mechanically induced defects which are a natural consequence of point contact spectroscopy.

The outline of the paper is as follows. In the first part the preparation procedure is described in detail. The following part is devoted to the structural and chemical characterization of the films. Finally first results on the transport properties of UPt_3 films deposited on different substrate materials are presented. There are very few publications dealing with the thin-film preparation of UPt_3 [14]. The results of these investigations reveal two main problems. First of all, the deposition processes used up to now resulted in polycrystalline films. Secondly there was no clear evidence for superconductivity in the samples. We will show in the following sections that it is possible to prepare strongly textured and even epitaxially grown UPt_3 thin films on suitable substrate materials. Above a strongly reduced superconducting transition temperature of 130 mK, as compared to 530 mK for bulk samples, epitaxially grown thin films show renormalized transport properties without evidence for heavy quasiparticles.

2. Preparation

The preparation of the UPt_3 films was performed in an UHV magnetron sputter system with a base pressure below 10^{-8} hPa (1 hPa = 100 Pa). High-purity argon (purity 6N) was used as the sputtering gas in the pressure range from 3×10^{-2} hPa to 7×10^{-2} hPa measured by a capacitive pressure gauge. The substrate was mounted on a rotatable holder driven by a computer-controlled stepper motor. By rotating the heated substrate between two targets of uranium (purity 3N, SICN Annecy, France) and platinum (purity 2N5, Leybold, Germany) and by varying the respective deposition times in front of the targets, the stoichiometry could be controlled within an accuracy of $\pm 5\%$. In order to secure the formation of the UPt_3 compound in this quasi-multilayer deposition technique the effective thickness of each deposited single layer was kept below two monolayers while the substrate was held at an elevated temperature. Within the typical sensitivity of 5% in the x-ray diffraction, no crystalline platinum or uranium could be detected for substrate temperatures above 580 K. Before the deposition process the substrate was heated above 1380 K for at least 20 min while a plasma discharge at the platinum and uranium target was maintained (pre-sputtering) in order to remove any degraded surface layer especially on the uranium target. After deposition, the cooling rate of the films was held at 20 K min^{-1} controlled by a computer. The structural quality of the samples was investigated by x-ray diffraction in Bragg–Brentano geometry on a standard two-circle diffractometer using Cu Kα radiation complemented by ϕ-scan measurements on a four-circle diffractometer. The composition of the films was determined by energy-dispersive x-ray spectroscopy, EDX (Link, OXFORD), within an accuracy of $\pm 1\%$. Information about the surface of the films was obtained by means of a scanning electron microscope (JSM-6300F, JEOL) and a scanning force microscope (TMX 2000, Topometrix). The growth characteristic of UPt_3 was investigated on single-crystalline substrates of Al_2O_3, $LaAlO_3$ and $SrTiO_3$ revealing in every case a growth preference with the c-axis of UPt_3 perpendicular to the substrate surface. X-ray diffraction and EDX indicated a more pronounced formation of impurity phases for uranium excess (UPt and UPt_2) and less
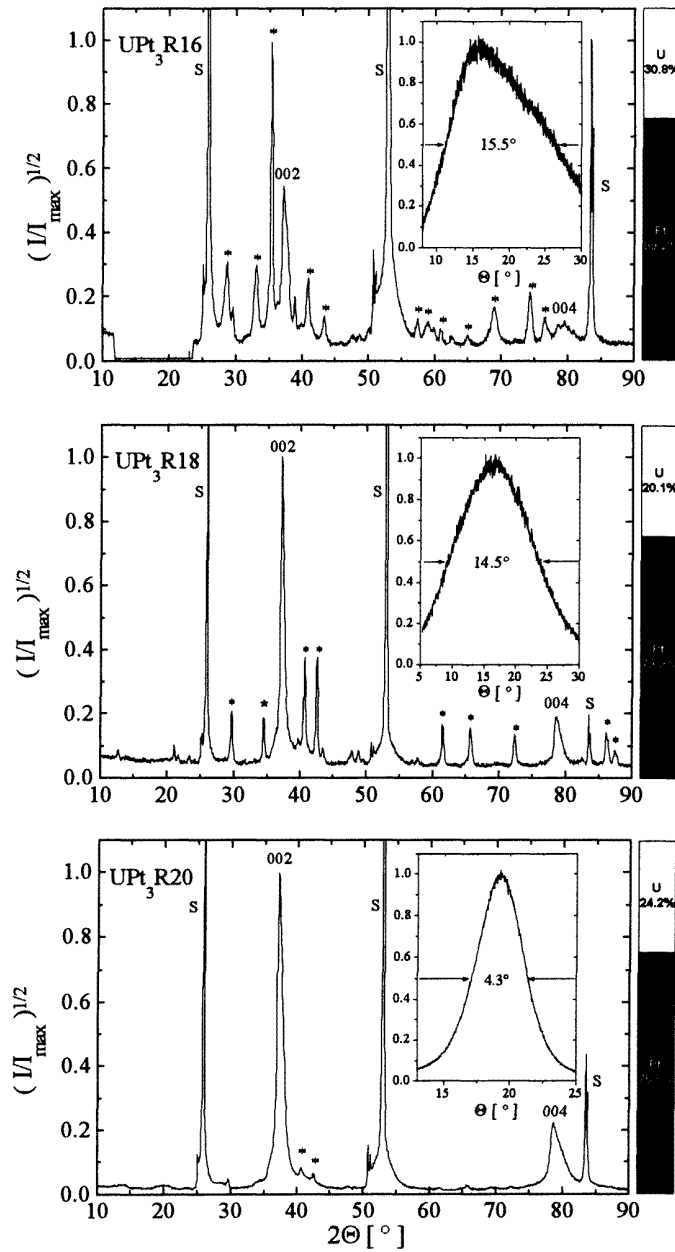
Figure 1. X-ray diffraction patterns in the Bragg–Brentano geometry for UPt_3 films on $Al_2O_3(10\bar{1}2)$. The respective uranium and platinum contents as deduced from EDX are indicated in the bar diagrams. Impurity phases are marked by asterisks.

impurity phase formation for uranium deficiency (UPt_5 and Pt). Quite independent from the substrate material, the optimized sputter parameters for the UPt_3 phase formation can be given as follows: argon partial pressure $p_{Ar} = 4 \times 10^{-2}$ hPa, sputter current for both
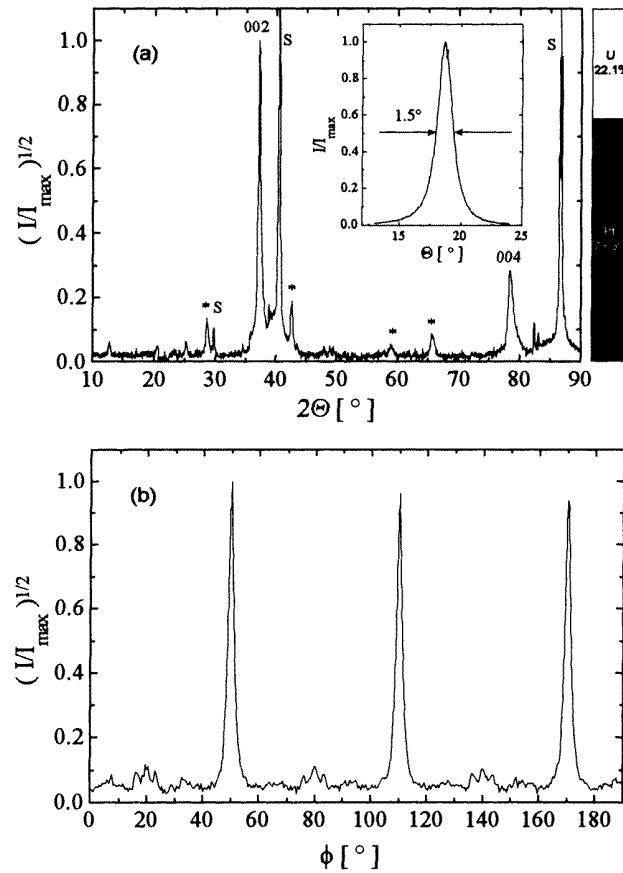
Figure 2. (a) An x-ray diffraction pattern in Bragg–Brentano geometry for an UPt$_3$ film on SrTiO$_3$(111). The respective uranium and platinum contents as deduced from EDX are indicated in the bar diagram. Impurity phases are marked by asterisks. (b) A ϕ-scan of the 201 reflection showing the in-plane order of the film.

targets $I = 20$ mA, substrate temperature during deposition $T_{sub} = 995 \pm 15$ K, ratio of respective deposition periods $t_U/t_{Pt} = 3.7$ s/6.0 s $\cdots$ 4.0 s/6.0 s.

Based on the residual resistance ratio $RRR = \rho(300 \text{ K})/\rho_0$, *in situ* annealing of the films after deposition gave no evidence for an improvement of the film quality on any of the substrate materials. Annealing above 1050 K resulted in a phase decomposition of the samples. Details concerning the influence of the substrate material and orientation on the UPt$_3$ phase formation are presented in the following section.

3. Structural characterization

3.1. Growth on Al$_2$O$_3$ and LaAlO$_3$

Despite the lack of compatibility of the twofold surface symmetry of Al$_2$O$_3$ in the $(10\bar{1}2)$ orientation (r-plane) and the sixfold basal-plane symmetry of UPt$_3$ in the c-axis
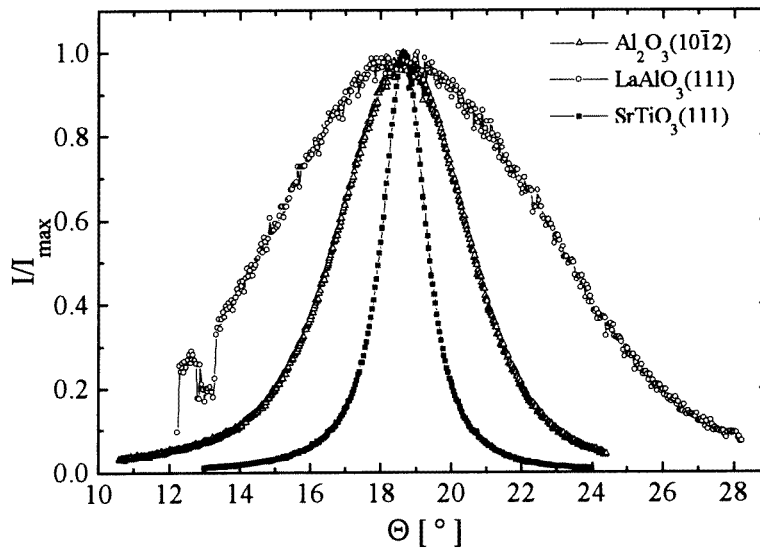
Figure 3. Rocking curves of the 002 reflection for UPt₃ films on different substrate materials and for different orientations.

growth direction, the phase formation of UPt₃ could be observed for an optimized sample composition. This can be seen in figure 1 which shows a comparison of the x-ray diffraction patterns for three films with different uranium-to-platinum ratios as deduced by EDX using a standard ZAF correction. The optimized UPt₃ phase purity is in clear correspondence with a nominal uranium composition of 25%. The growth on Al_2O_3 in the *r*-plane orientation is strongly textured with a *c*-axis growth preference. In correspondence with the lack of symmetry compatibility at the interface, a ϕ-scan of the 201 reflection revealed no in-plane order of the films.

Similar results were obtained on $LaAlO_3$ in a (111) orientation that should support the intrinsic growth preference due to the threefold symmetry of the $LaAlO_3$(111) plane. Nevertheless, no evidence for an improved structural quality of the samples as compared to Al_2O_3 was found, which is most probably due to the large lattice misfit of -7%. Further characterization concerning a possible in-plane orientation was not performed.

3.2. Growth on $SrTiO_3$

In order to support an in-plane order of the films, $SrTiO_3$ in the (111) orientation (threefold symmetry) was used as the substrate material (see figure 2). In spite of the rather large lattice misfit of $+4.3\%$, epitaxial growth of UPt₃ was induced as can be seen in figure 2(b). The misfit values refer to room temperature. Since lattice constants and thermal expansion coefficients of UPt₃ are not available at the growth temperature, a crude estimation of the resulting misfit during growth can be given based on the thermal expansion coefficient at 100 K. According to experiments by de Visser *et al* [16] the thermal expansion coefficient at 100 K already shows a saturation tendency reaching roughly 10×10^{-6} K^{-1}. With a thermal expansion coefficient of 9.4×10^{-6} K^{-1} for $SrTiO_3$ and a Debye temperature $\Theta \simeq 400$ K the misfit will only be modified in the pro mille region up to 1000 K. The width of the rocking curves for films deposited on different substrate materials and orientations corroborates the

conclusion that $SrTiO_3(111)$ is an epitaxial substrate for UPt_3 in the (0001) growth direction (see figure 3). The optimum full width at half-maximum of 1.5° that was achieved on $SrTiO_3(111)$ leaves room for further improvement.

3.3. The influence of the sputtering parameters

In the following section, an overview concerning the influence of variations of the sputtering parameters on the phase formation and morphology of the films is given.
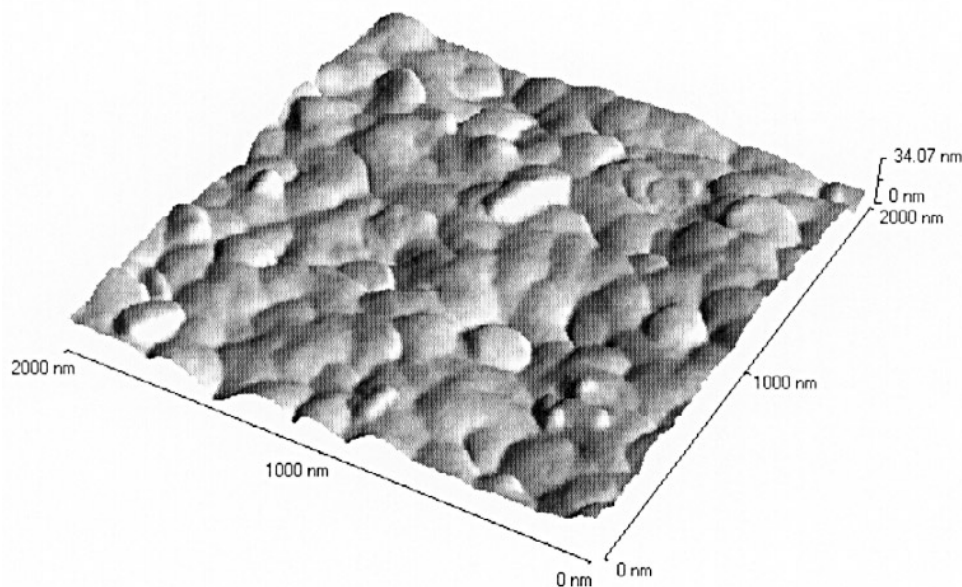

Figure 4. An atomic force microscopy image of a UPt_3 film on $SrTiO_3(111)$ (sample No 94).

Independently of the various sputtering parameters, like sputtering gas pressure, substrate temperature and the respective deposition times, the formation of UPt_3 could only be observed for sputter currents above 15 mA on both targets with an optimized value of 20 mA. The investigation of the surface morphology of the films by atomic force microscopy gave evidence for an island growth mode with a typical island size of 200–500 nm and a typical height variation of 12 nm (see figure 4). The interpretation of the surface morphology as evidence for an island growth mode will be further corroborated in the following section. On reducing the sputtering current below 15 mA, in conjunction with the lack of UPt_3 phase formation, the surface of the films become smoother with reduced island sizes in the range 50–100 nm. Consequently the mean island diameter of 350 nm as observed for high-quality samples seems to be typical for the UPt_3 phase. The parallel reduction of the sputtering voltage for a reduced current should result in a lower kinetic energy of the sputtered metal clusters and atoms. Thereby the surface mobility of the adatoms could be too low for UPt_3 phase formation.

The variation of the substrate temperature during deposition revealed the tendency for UPt_3 growth in the range from 920 K to 1060 K ($I = 20$ mA, $p_{Ar} = 4 \times 10^{-2}$ hPa). The optimum growth was observed for substrate temperatures in the interval $T_{sub} = 995 \pm 15$ K.

The influence of the sputtering gas pressure on the phase formation was investigated in the range 2×10^{-2} hPa $\leqslant p_{Ar} \leqslant 7 \times 10^{-2}$ hPa showing an optimum value around 4.0×10^{-2} hPa.
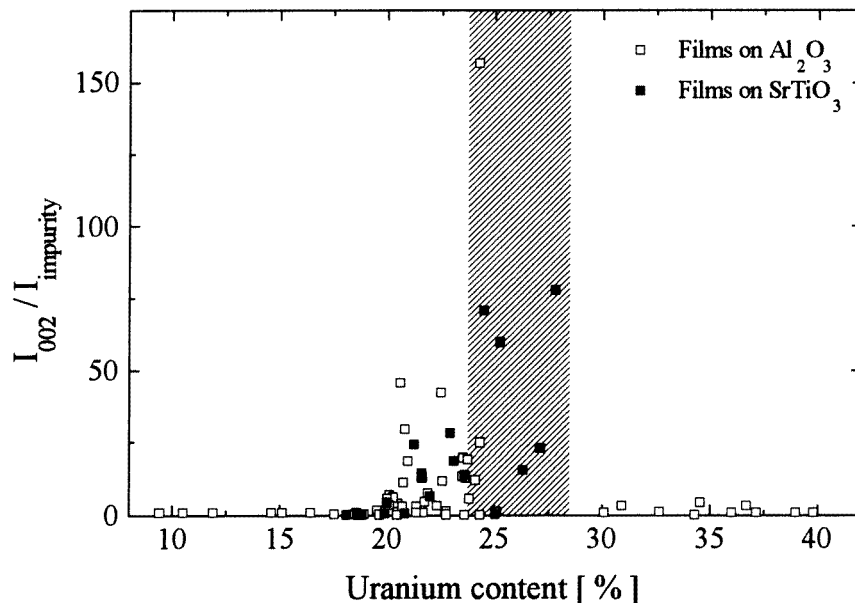

Figure 5. The growth preference of the (0001)-oriented UPt₃ phase as a function of the uranium content (deduced from EDX). $I_{impurity}$ and I_{002} denote the intensity of the most prominent impurity phase Bragg reflection and the intensity of the UPt₃ 002 reflection respectively. The hatched region characterizes the region of dominating UPt₃ phase formation.

As a rough measure of the UPt₃ phase purity figure 5 shows the ratio of the respective intensities of the largest Bragg reflection of UPt₃ (i.e. 002) and the most prominent impurity phase as a function of the overall uranium content that was estimated by EDX for several films on Al₂O₃ and SrTiO₃. An almost pure UPt₃ phase formation was found in the rather small uranium content interval from 23% to 28% with a tendency for an increased phase formation in the uranium-depleted region (20% to 23%). The resulting necessary precision in the respective deposition times is at the limit of the achievable accuracy within the deposition method used.

Concluding the aspects of structural characterization, UPt₃ was deposited epitaxially in the (0001) orientation on SrTiO₃(111) substrates whereas only textured growth could be observed on the Al₂O₃ r-plane. The mosaicity of films on SrTiO₃(111) is strongly improved (1.5°) as compared to a typical full width at half-maximum of at least 4° on Al₂O₃. The surface morphology gives evidence for an island growth mode. A more thorough discussion of the growth mode will be taken up in the next section in conjunction with the microstructure–transport property relationship.

4. Transport properties

The temperature-dependent resistivity $R(T)$ for UPt₃ films on the Al₂O₃ r-plane is in good qualitative correspondence with the typical $R(T)$-curve of bulk samples [15]. A
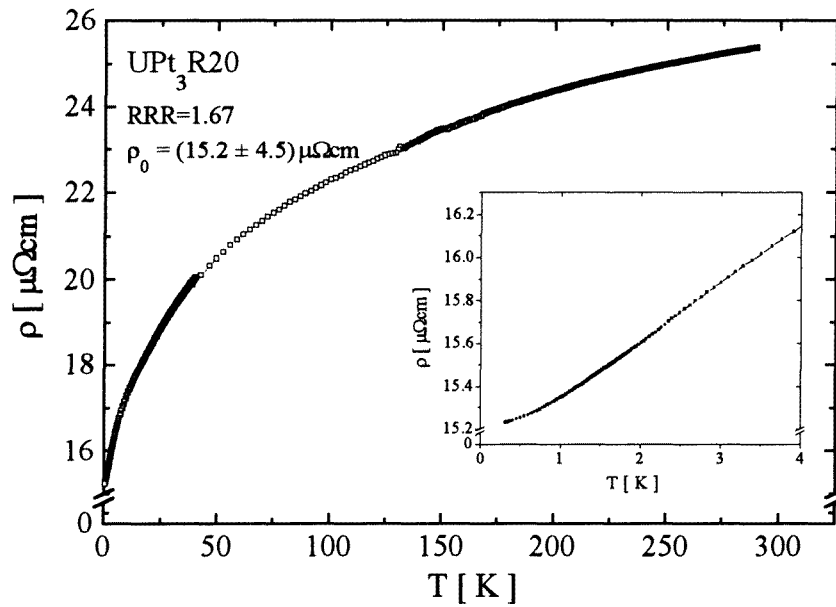
Figure 6. The temperature-dependent specific resistivity for a UPt₃ film on Al₂O₃(10$\bar{1}$2). The current is perpendicular to the film's *c*-axis.

representative result is shown in figure 6. Nevertheless, there are some discrepancies worth mentioning. The specific resistivity at room temperature is reduced by a factor of 6 to 7 as compared to typical values measured on bulk samples. The residual resistance ratio is exceptionally low ($RRR \simeq 2$). Down to the lowest measured temperature of 300 mK no superconducting transition was found.

Unlike the results for films on Al₂O₃, the $R(T)$-characteristics of UPt₃ films on SrTiO₃ show almost no resemblance to the resistance curves of bulk samples. The room temperature specific resistivity is even further reduced as compared to that of bulk samples by a factor of 12 (see figure 7). The residual resistivity ratio reaches values up to 930 in some of the films and 612 for the sample shown. A resistivity measurement down to the millikelvin range revealed a superconducting transition at about 130 mK (the midpoint). Typical transition temperatures in bulk samples are in the region of 500 mK.

Since the overall $R(T)$-characteristics for films on SrTiO₃ show no evidence for the development of a heavy-quasiparticle band at low temperatures, several possible reasons have to be taken into account. The preparation method is based on a multilayer deposition technique which could result in a layered structure of uranium and platinum. As a consequence, the very low specific resistivity could be caused by a short-circuit effect due to a current channelling in the platinum layers, whereas the superconducting transition could be caused by the uranium layers. Several experimental results exclude this possibility. Due to the rather large deposition temperature (1000 K) a strong tendency for interdiffusion of uranium and platinum can be expected. X-ray diffraction does not reveal any evidence for elemental uranium or platinum, nor is there any hint for an artificial superstructure. A calculation of the course of the resistivity for a parallel circuit of platinum and uranium yielded no correspondence with the observed temperature-dependent resistivity of the films. In order to observe superconductivity of uranium the impurity phase content must exceed the
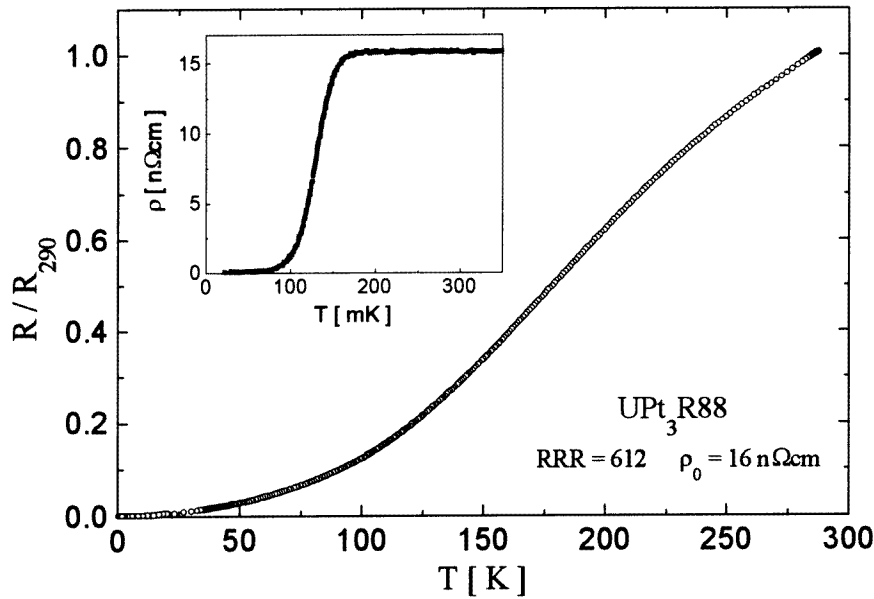
Figure 7. The temperature-dependent resistivity normalized to the value at 290 K for a UPt_3 film on $SrTiO_3(111)$. The current is perpendicular to the film's c-axis. The onset of superconductivity is shown in the inset.

percolation limit and should thus be detectable in x-ray diffraction. A clear-cut experiment to exclude phase segregation or parasitic superstructure effects would be given by cross section TEM studies. Especially in the near-interface region, TEM studies could help to distinguish between a true island growth mode and Stranski–Krastanov growth which would result in a more pronounced relaxation of strain in the films. Such experiments could not be performed up to now.

We propose the growth mode itself as the reason for the strongly renormalized resistivity behaviour for films on $SrTiO_3$. Recent results concerning intrinsic stress measurements for metal films on several substrate materials give clear evidence for the development of lateral compression for those films that grow in an epitaxial Vollmer–Weber mode (island growth) [17, 18]. Such a domain compression effect is due to a reciprocal effect of epitaxial growth despite a lattice misfit at the film–substrate interface and the coalescence of the film islands that takes place without the formation of grain boundaries. This scenario is corroborated by several experimental findings on the UPt_3 films on $SrTiO_3$. The epitaxial Vollmer–Weber growth is typically observed for high substrate temperature during deposition. X-ray diffraction of the films reveals a high degree of in-plane order. Furthermore, due to the very large residual resistance ratios the existence of an appreciable density of grain boundaries seems not to be very probable. Here again, TEM studies could help to corroborate or disprove this assumption. The renormalization effects on the electronic properties of UPt_3 bulk samples under quasi-hydrostatic pressure result in a reduction of the room temperature resistivity of approximately 30% at 200 kbar [19]. The resulting course of the resistivity in the bulk samples as a function of temperature is in good correspondence with the data presented for the films. The large reduction of the resistivity at room temperature in the films by one order of magnitude as compared to that of bulk samples could be due to

anisotropies of the elastic constants that were already proven to arise in uniaxial pressure experiments on single-crystal whiskers with the current along the expanded c-axis [20]. To our knowledge no experiments with uniaxial expansion along the c-axis (corresponding to compressive strain in the ab-plane) and a current flow perpendicular to the c-axis have been performed up to now in the pressure regime above 150 kbar. In the low-temperature part of the resistivity, no increase of the coefficient A in the typical Fermi liquid behaviour $\rho(T) = \rho_0 + AT^2$ was found. In some of the films on SrTiO$_3$, even a slight increase of the resistivity below 1 K could be observed. The reduction of the T^2-coefficient by more than one order of magnitude (0.6 $\mu\Omega$ cm at ambient pressure, <50 nΩ cm at 200 kbar) was also found in quasi-hydrostatic pressure experiments on a UPt$_3$ whisker [19].

Further experiments will concentrate on several aspects in order to corroborate the above conclusions about the influence of lateral compressive strain. The influence of the misfit between the UPt$_3$ films and the substrate will be elucidated by investigations of the growth on MgO(111) (misfit $(a_{\mathrm{UPt_3}} - a_{\mathrm{sub}})/a_{\mathrm{UPt_3}} = -3.1\%$ as compared to $+4.3\%$ for films on SrTiO$_3$(111)). In order to scrutinize the microstructure–property relationship in more detail, we will attempt to supplement the structural characterization of the films on different substrate materials with various lattice misfits by means of cross section TEM studies. Finally, experiments concerning the influence of lateral expansion on the temperature-dependent resistivity of UPt$_3$ films on SrTiO$_3$(111) are in progress.

Acknowledgment

References

[1] Fulde P, Keller J and Zwicknagl G 1988 *Solid State Commun.* **41** 1
[2] Sauls J A 1994 *Adv. Phys.* **43** 113
[3] von Löhneysen H 1994 *Physica* B **197** 551
[4] Adenwalla S, Lin S, Ran Q, Zhao Z, Ketterson J, Sauls J, Taillefer L, Hinks D, Levy M and Sarma B 1990 *Phys. Rev. Lett.* **65** 2298
[5] Hasselbach K, Taillefer L and Flouquet J 1989 *Phys. Rev. Lett.* **63** 93
[6] Fisher R A, Kim S, Woodfield B F, Phillips N E, Taillefer L, Hasselbach K, Flouquet J, Giorgi A L and Smith J L 1989 *Phys. Rev. Lett.* **62** 1411
[7] Shivaram B S, Jeong Y H, Rosenbaum T F and Hinks D G 1986 *Phys. Rev. Lett.* **56** 1078
[8] Trappmann T, von Löhneysen H and Taillefer L 1991 *Phys. Rev.* B **43** 13714
[9] von Löhneysen H, Trappmann T and Taillefer L 1992 *J. Magn. Magn. Mater.* **108** 49
[10] Hayden S M, Taillefer L, Vettier C and Flouquet J 1992 *Phys. Rev.* B **46** 8675
[11] Machida K and Ozaki M 1991 *Phys. Rev. Lett.* **66** 3293
[12] Chen D and Garg A 1993 *Phys. Rev. Lett.* **70** 1689
[13] Wollman D A, van Harlingen D J, Lee W C, Ginsberg D M and Leggett A J 1993 *Phys. Rev. Lett.* **71** 2134
[14] Holter G E and Adrian H 1986 *Solid State Commun.* **58** 45
       Kang J 1987 *PhD Thesis* Minneapolis University
       Adrian G E and Adrian H 1989 *J. Less-Common Met.* **149** 313
[15] See, for example,
       Brison J P, Keller N, Lejay P, Tholence J L, Huxley A, Bernhoeft N, Buzdin A I, Fåk B, Flouquet J, Schmidt L, Stepanov A, Fisher R A, Phillips N and Vettier C 1994 *J. Low Temp. Phys.* **95** 145
[16] de Visser A, Franse J J M and Menovsky A 1985 *J. Physique Lett.* **15** L53
[17] Koch R, Winau D, Thürmer K, Weber M and Rieder K H 1993 *Europhys. Lett.* **21** 213
[18] Koch R 1994 *J. Phys.: Condens. Matter* **6** 9519
[19] Ponchet A, Mignot J M, de Visser A, Franse J J M and Menovsky A 1986 *J. Magn. Magn. Mater.* **54–57** 399
[20] Taillefer L, Flouquet J, Gaidukov Y P and Danilova N P 1992 *J. Magn. Magn. Mater.* **108** 138